European Polymer Journal 45 (2009) 2211–2221

Contents lists available at ScienceDirect

European Polymer Journal

journal homepage: www.elsevier.com/locate/europolj

Characterization and properties of a polythiophene with a malonic acid dimethyl ester side group

Elaine Armelin [a,b,1], Oscar Bertran [c,1], Francesc Estrany [b,d], Roser Salvatella [d], Carlos Alemán [a,b,*]

[a] Departament d'Enginyeria Química, E.T.S. d'Enginyers Industrials de Barcelona, Universitat Politècnica de Catalunya, Diagonal 647, Barcelona E-08028, Spain
[b] Center for Research in Nano-Engineering, Universitat Politècnica de Catalunya, Campus Sud, Edifici C', C/Pasqual i Vila s/n, Barcelona E-08028, Spain
[c] Departament d'Enginyeria Química, EUETII, Universitat Politècnica de Catalunya, Pça Rei 15, Igualada 08700, Spain
[d] Unitat de Química Industrial, EUETIB, Universitat Politècnica de Catalunya, Comte d'Urgell 187, Barcelona 08036, Spain

ARTICLE INFO

Article history:
Received 3 February 2009
Received in revised form 12 May 2009
Accepted 21 May 2009
Available online 27 May 2009

Keywords:
Conducing polymers
Polythiophene
Malonic acid
Quantum mechanics

ABSTRACT

A new polythiophene derivative bearing a malonic acid dimethyl ester substituent attached to the 3-position of the repeat unit has been prepared by chemical oxidative-coupling polymerization. The chemical structure of poly(2-thiophen-3-yl-malonic acid dimethyl ester) has been analyzed by FTIR and ^{1}H NMR spectroscopy and, additionally, the distribution of the head-to-tail and head-to-head diads arising from polymerization was found to be a 75–25%. The glass transition temperature identified for this polymer was 17.6 °C lower than that recently determined for a closely related polythiophene derivative, in which the ester substituent arose from acrylic acid rather than from malonic acid. On the other hand, the electrical conductivity of the new material, which was soluble in polar solvents but not in water, was higher than that typically found for poly(3-alkylthiophene) derivatives. Ab initio quantum mechanical calculations on simple model compounds were used to predict the regiochemistry of the polymer chain, which was in excellent agreement with the experimental observation, and the conformational preferences of both the inter-ring dihedral angle and the bulky side group. Interestingly, calculations predict that the inter-ring dihedral angles adopt a *syn-gauche* conformation rather than the *anti-gauche* arrangement typically found in substituted polythiophenes. Thus, in this case the former conformation reduces the strong repulsive interactions induced by the bulky substituent. The lowest π–π^* transition energy derived from calculations on an idealized molecular model is in agreement with the experimental estimation determined using UV–vis spectroscopy. This electronic property is significantly higher for poly(2-thiophen-3-yl-malonic acid dimethyl ester) than for other substituted polythiophene derivatives, which is consequence of the geometrical distortions induced by bulky side group.

1. Introduction

Much progress has been made in the past decades to solve the serious problems of solubility and processability of thiophene-based functional conducting polymers [1–3]. This problem was overcome by the incorporation of substituents to the 3-position of the thiophene ring, which produced not only processable conducting polymers but also allowed the complete chemical and physical characterization of the prepared materials [4–6]. Specifically, it was found that the introduction of long alkyl side chains increases the solubility in organic solvents, whereas hydrophilic substituents produce polythiophenes soluble in water and/or polar solvents.

We are particularly interested in the development of soluble polythiophenes with electron-withdrawing carboxylic acid groups in the 3-position of thiophene ring.

* Corresponding author. Address: Departament d'Enginyeria Química, E.T.S. d'Enginyers Industrials de Barcelona, Universitat Politècnica de Catalunya, Diagonal 647, Barcelona E-08028, Spain. Tel.: +34 93 401 08 83; fax: +34 93 401 71 50.
E-mail address: carlos.aleman@upc.edu (C. Alemán).
[1] Both authors contributed equally to this work.

0014-3057/$ - see front matter © 2009 Elsevier Ltd. All rights reserved.
doi:10.1016/j.eurpolymj.2009.05.024

Within this field, the pioneering work of Heeger and coworkers [7] in polythiophenesulfonates was one of the most important contributions to water-soluble conducting polymers influencing subsequent research in this field. For example, Chayer et al. [8] reported a highly conducting polythiophene derivative based on sodium poly [2-(3-thienyloxy)ethanesulfonate] and sodium poly[2-(4-methyl-3-thienyloxy)ethanesulfonate], while Masuda and Kaeriyama [9] provided the synthesis of the water-soluble sodium salt of poly(thiophene-3-carboxylate). Electroactive polymers and copolymers with acetic acid, propionic acid and octanoic acid linked to thiophene ring have been also investigated [10–14]. On the other hand, we recently reported the synthesis, structural and electronic characterization of poly(3-thiophen-3-yl-acrylic acid methyl ester) and poly(3-thiophene-3-yl acrylic acid) (PT3AME and PT3AA, respectively) [15,16]. Unfortunately, these materials were not soluble in water as we initially expected, even although they were soluble in polar solvents ensuring their processability. Being the development of polythiophene derivatives soluble in water very important because of the potential biotechnological applications of these materials [17–19], the solubility in strong polar solvents having high boiling points is also of great importance because of the improvement in the processability.

Attracted by this field, in this work we report a comprehensive experimental and theoretical study about the properties of poly(2-thiophen-3-yl-malonic acid dimethyl ester) (abbreviated PT3MDE), a new polythiophene derivative bearing a substituent with two carboxylate groups per structural unit (Scheme 1) that has been prepared by chemical oxidative-coupling polymerization. The more relevant properties of this material have been characterized by FTIR, NMR and UV–vis spectroscopy, TGA and DSC, electrical measurements and theoretical calculations. Results have been compared with those obtained for other polythiophenes bearing substituents with polar groups. It should be noted that we recently found that polythiophene derivatives bearing polar side groups, as for example PT3AME, are able to form specific interactions with plasmid DNA [17–19]. Accordingly, the new conducting polymer reported in this work should be considered as another promising template for the future development of specific DNA sensors.

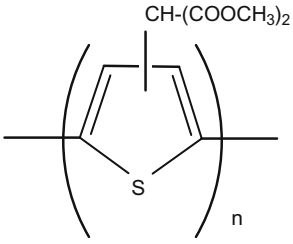

PT3MDE

Scheme 1.

2. Methods

2.1. Chemicals

2-Thiophen-3-yl-malonic acid (T3MA) and anhydrous ferric chloride were purchased from Sigma–Aldrich S.A., being employed without further purification. All solvents were purchased from Panreac Química S.A. with ACS grade.

2.2. Equipments

FTIR spectra were recorded on a FTIR 4100 Jasco spectrophotometer. The samples were placed in an attenuated total reflection accessory with thermal control and a diamond crystal (Specac model MKII Golden Gate Heated Single Reflection Diamond ATR). Proton NMR spectra were recorded on a Varian Inova 300 spectrometer operating at 300.1 MHz. Both the monomer and the polymer were dissolved in deuterated chloroform ($CDCl_3$), and the chemical shifts (δ) were calibrated using tetramethylsilane as internal standard. The thermal behavior of PT3MDE was examined by differential scanning calorimetry (DSC) using a Perkin–Elmer DSC Pyris 1 calibrated with indium metal. DSC data were obtained from samples of 5–8 mg at heating/cooling rates of 10 or 20 °C/min^{-1} under a flow of dry nitrogen. Thermogravimetric analyses (TGA) were carried out with a Perkin–Elmer TGA-6 thermobalance at a heating rate of 20 °C/min under a nitrogen atmosphere. The UV–vis optical spectrum of the polymer was obtained from its 1 mg/mL solution in acetone using a Shimatdzu UV-240 Graphtcord UV–vis recording spectrophotometer.

2.3. Theoretical calculations

Full geometry optimizations of oligomers containing n monomeric units (n-T3MDE) with n ranging from 1 to 6 were performed using the Hartree–Fock method combined with the 6-31G(d,p) basis set [20], i.e. HF/6-31G(d,p) level. Previous studies indicated that this simple methodology is able to provide a very satisfactory description of the molecular geometry and relative energy for the minimum energy conformations of heterocyclic oligomers like those studied in this work [21,22]. Calculations on n-T3MDE oligomers were carried out considering both the *anti-gauche* ($\theta \approx 145°$) and *syn-gauche* ($\theta \approx 40°$) conformations as starting structures, the inter-ring dihedral angle θ being defined by sequence S–C–C–S. Thus, previous studies on disubstituted 2,2′-bithiophene derivatives indicated that these conformations are relatively close to those typically identified as the global and the local minima, respectively [23,24].

The Koopmans' theorem [25] was used to estimate the ionization potentials (IPs). Accordingly, IPs were taken as the negative of the highest occupied molecular orbital (HOMO) energy, i.e. IP = $-\varepsilon_{HOMO}$. The IP indicates if a given acceptor (p-type dopant) is capable of ionizing, at least partially, the molecules of the compound. The $\pi-\pi^*$ lowest transition energy (ε_g) was approximated as the difference between the HOMO and lowest unoccupied molecular orbital (LUMO) energies, i.e. $\varepsilon_g = \varepsilon_{LUMO} - \varepsilon_{HOMO}$. Although HF calculations provide a satisfactory qualitative descrip-

tion of the electronic properties of polyheterocyclic molecules, we are aware that this method tends to overestimate the values of IP and ε_g [26,27]. Accordingly, the electronic properties presented in this work have been estimated performing single point Density Functional Theory (DFT) calculations with the B3PW91 [28,29] method combined with the 6-31G(d,p) basis set [30], i.e. B3PW91/6-31G(d,p), on the molecular geometries optimized at the HF/6-31G(d,p) level. Electronic properties predicted by this methodological combination and experimental values are expected to be quantitatively comparable. Thus, previous studies on π-polyconjugated systems indicated that the B3PW91 functional is able to reproduce very satisfactorily a wide number of electronic properties [15,16,22,31,32]. It is worth noting that according to the Janaks theorem [33], the approximation mentioned above for the calculation of the IP can be applied to DFT calculations, while Levy and Nagy evidenced that ε_g can be rightly approximated as the difference between ε_{LUMO} and ε_{HOMO} in DFT calculations [34].

All the quantum mechanical calculations presented in this work were performed using the Gaussian 03 computer program [35].

3. Results and discussion

3.1. Synthesis

PT3MDE was prepared by oxidative-coupling polymerization (Scheme 2) using the procedure described by Sugimoto and coworkers [36], which was successfully employed to synthesize other polythiophene derivatives containing different polar pending groups [15,16]. For this purpose, the 2-thiophen-3-yl-malonic acid dimethyl ester (T3MDE) monomer was obtained (90% of yield) by refluxing T3MA (3 g) in dry methanol (15 mL) with one-two drops of concentrated sulfuric acid for 24 h. The purification of T3MDE was carried out by the evaporation of methanol and successive extraction with diethyl ether. The extract was washed with distilled water, dried with anhydrous $MgSO_4$, and filtered washing several times with diethyl ether. The product was recovered after solvent evaporation under reduced pressure.

Chemical polymerization of T3MDE was performed by chemical oxidative-coupling in dry chloroform using anhydrous ferric chloride. In a 200 mL three-necked flask, 80 mmol of ferric chloride was dissolved in 60 mL of dry chloroform under nitrogen and stirred. Next, a solution of 20 mmol of monomer in 40 mL of chloroform was added dropwise. As was recommended by Sugimoto and coworkers when the oxidant is ferric chloride, the oxidant:monomer molar ratio was 4:1 [36]. The mixture was stirred for 24 h and after stored in the freezer overnight. Thus, we poured out the dark-blue doped polymer into a large excess of methanol (2 L) in order to precipitate the PT3MDE. The color of the resulting product changed to dark-red, respectively, when poured into methanol. The precipitated polymer was recovered in chloroform and successively washed with methanol to remove the residual $FeCl_3$, the residual monomer and small oligomers. After drying under vacuum at 40 °C for 72 h, product was obtained with a yield between 60 and 75%. Unfortunately, determination of the molecular weight of the polymer by GPC analysis using polystyrene standards and hexafluoro-2-propanol as solvent was not possible. Similarly, MALDI-TOF mass spectrometry analyses in several types of matrices (dihydrobenzoic acid, dithranol, sinapinic acid, etc.) gave variable and inaccurate results. Therefore, the yield value was estimated according to the weight mass obtained.

3.2. Structural characterization

The FTIR spectra of Fig. 1 show the main absorption bands for the T3MA and T3MDE monomers and the polymer studied in this work. Detailed analysis of the absorption bands allowed us to confirm that the polymer was successfully obtained by chemical oxidative reaction with $FeCl_3$. Unsaturated compounds are typically detected by the bands higher than 3000 cm^{-1}. According to Ruiz et al. [37] the absorbance due to the aromatic C–H stretch at ~3070 cm^{-1} should be attributed to the β-hydrogen whereas the band at ~3090 cm^{-1} is related to the α-hydrogen position in the thiophene ring (Table 1). These absorbances could not be identified in the T3MA spectrum because of the broad band from the OH group detected between 3300 and 2500 cm^{-1}. On the other hand, the β C–H out-of-plane deformation is typically observed as a medium peak at about 850–870 cm^{-1} while the α C–H out-of-plane deformation appears as a very sharp band at 790–760 cm^{-1}. For the T3MA and T3MDE monomers these bands are observed at 785 and 798 cm^{-1}, respectively. As we can be seen in FTIR spectrum of the polymer, the strong peak at about 770 cm^{-1} (α C–H out-of-plane deformation) disappears indicating that the α positions of the thiophene ring have been successfully linked. On the other hand, two sharp bands, which correspond to the free C=O stretching (at 1751 cm^{-1}) and C=O associated forming hydrogen bonds (at 1657 cm^{-1}), can be appreciated for T3MA in Fig. 1. Therefore, the presence of the acid group and further esterification reaction was clearly detected in the carbonyl absorption region. The peak at 1740 cm^{-1} was attributed

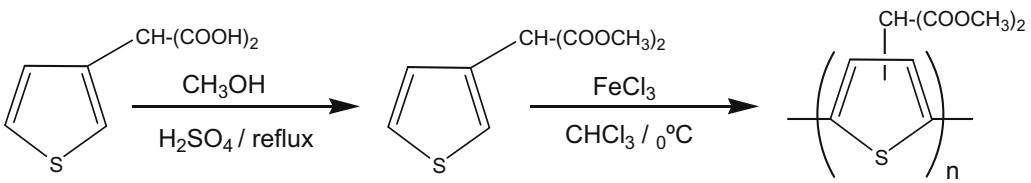

Scheme 2.

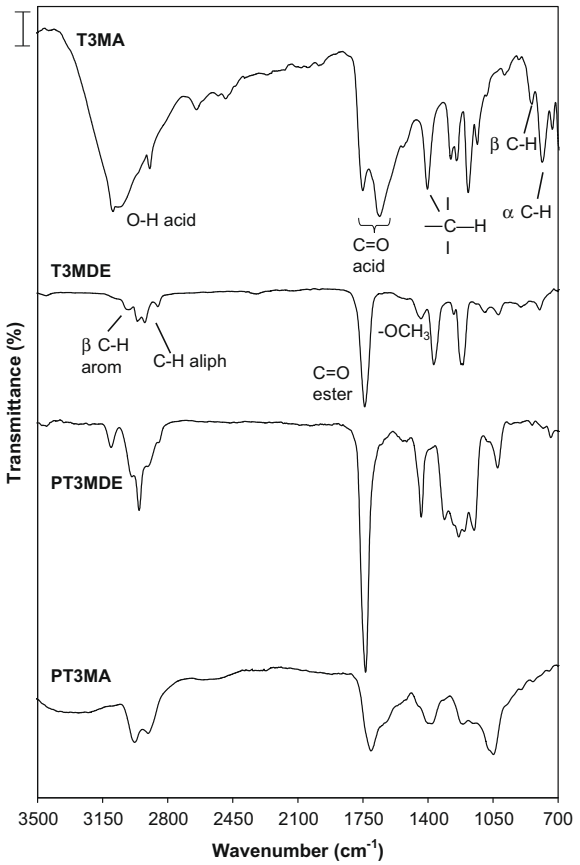

Fig. 1. FTIR-ATR spectra of T3MA and T3MDE monomers and PT3MDE polymer. Scale = 20% of transmittance.

to the C=O stretching vibration of ester from T3MDE, while the C–O stretching and the CH_3 asymmetric bending were detected at around 1200 and 1438 cm^{-1}, respectively.

The effect of polymerization can be recognized as a general broadening and overlapping of the absorption bands, which is partially accentuated by the presence of additional elements in the polymer chains, i.e. dopant ions and metals [38]. In spite of this, an approach in terms of chemical groups was interpreted. The main IR absorption bands for the thiophene derivatives are summarized in Table 1, a comparison with other related conducting polymers like poly(3-thiophene acetic acid) (P3TAA) [10], poly(3-hexylthiophene) (PHT) [39], and poly[3-(ethylmercapto)thiophene] (PEMT) [37] being also displayed.

The ^1H NMR spectra of T3MA, T3MDE and PT3MDE were in agreement with their expected chemical structures (Fig. 2): T3MA ($CDCl_3$) δ 12.52 ppm (s, –COO*H*, 1H), 7.26–7.11 ppm (m, thiophene protons, 3H), 4.86 ppm (s, aliphatic –*CH*–, 1H); T3MDE ($CDCl_3$) δ 7.26–7.11 ppm (m, thiophene protons, 3H), 4.86 ppm (s, aliphatic –*CH*–, 1H), 3.72 ppm (s, –COOCH_3, 6H); PT3MDE ($CDCl_3$) δ 7.33–7.17 ppm (thiophene protons, 1H), 4.79 ppm (aliphatic –*CH*–, 1H), 3.79, 3.62 ppm (–COOCH_3 split, 6H).

The esterification step was confirmed by the corresponding appearance of –$COOCH_3$ signal. As can be seen in Fig. 2, the ester groups of T3MDE were not deteriorated during the oxidative polymerization (peak at 3.7–3.6 ppm on PT3MDE spectra) [9]. General spectral broadening was observed as a result of the polymerization process, as expected. While the absence of any new peak after the polymerization step suggests the expected α–α coupling of the thiophene units, the presence of shoulders should be due to remaining α–H at the ring proton multiple region. This is usually associated to low molecular weight polymer molecules. On the other hand, splitting of the –$COOCH_3$ signal gives information about the ratio of head-to-tail (HT) and head-to-head (HH) diads arising from polymerization [40]. For poly(3-dodecylthiophene) the resonance for a HH coupling is observed at δ = 2.56 ppm while that of a HT coupling appears at δ = 2.79 ppm (protons on the α-carbon of the 3-position) [40]. Similarly, the relative ratio of HT–HH coupling for the polymers prepared in this work was determined by an accurate analysis of the protons from 3.7 to 3.0 ppm region in the ^1H NMR spectra. Analyses of peak areas (Fig. 2c, *e* and *e*′ protons) polymers showed a 75–25% distribution of these diads.

3.3. Thermal properties

DSC of PT3MDE was performed following a protocol that involves four scans: (i) a heating run of the sample at 10 °C/min as obtained from polymerization process; (ii) a cooling run of the sample at 10 °C/min; (iii) a second heating run at 10 °C/min to obtain melt transition; and (iv) a third heating run at 20 °C/min after quench the sample in liquid nitrogen. DSC scans from 0 to 300 °C at 10 °C/min were absent of endotherm transitions. Accordingly, we concluded that PT3MDE is completely amorphous. However, the glass transition temperature was observed at around −20.1 °C, after fast cooling at −60 °C and subsequently heating at 20 °C/min (Fig. 3a). This temperature is lower than that obtained for PT3AME, −2.5 °C [15], indicating that the flexibility of the polythiophene chain is higher when the ester substituent arises from malonic acid than from acrylic acid.

TGA was performed scanning from 30 to 700 °C at 20 °C/min. Fig. 3b shows that the decomposition of PT3MDE takes place through a two-steps process. However, the thermal cleave of the carboxylic ester moiety, which has been observed in other cases [41], is not involved in these steps because the mass loss does not correspond to the weight of methanol residues. Thus, we attributed such degradation process to the whole polymer. Specifically, the TGA curve shows a pronounced fall between 170 and 400 °C and a slight shoulder between 400 and 550 °C. The remaining weight percentage, which corresponds to inorganic residues contained in the conducting system, was 18% at 700 °C.

3.4. Solubility and electrical conductivity

PT3MDE is soluble in polar solvents such as chloroform, tetrahydrofuran, dimethyl sulfoxide, acetone and dichloroacetic acid. However, this polythiophene derivative is completely insoluble in hydroxylated solvents, such as ethanol and pentanol, and in water. Unfortunately, the insolubility

Table 1
Main infrared absorption bands (cm^{-1}) for the monomers (T3MA and T3MDE) and the polymer (PT3MDE) studied in this work. Data reported in the literature for related conducting polymers have been included for comparison.

Compound Abrev.	Aromatic C–H in plane deform.		Aliphatic C–H stretch	C=O acid or ester	C=C conjugated diene	CH_3 asymmetric. bending	C–O stretches	Aromatic C–H out-of-plane bending	Aromatic C–H out-of-plane deform.	
	α	β							α	β
T3MA	–	–	–	1751, 1657	–	–	1183, 1244	–	785	840
T3MDE	–	–	2923, 2853	1740	–	1438	1261, 1214	–	798	896
PT3MDE	–	3105	2952, 2850	1736	–	1437	1234, 1153	–	–	839
P3TAA[a]	~3000		3000–2800	1700	–	1410	~1200	–	–	836
PHT[b]	–	3055	2959, 2858	–	1512, 1458, 1439	1377	–	–	–	825
PEMT[c]	3090	3070	2974, 2867	–	1508, 1481, 1423	1373	–	–	–	825

[a] P3TAA: poly(3-thiophene acetic acid) (P3TAA). From Ref. [10].
[b] PHT: poly(3-hexylthiophene). From Ref. [36].
[c] PEMT: poly[3-(ethylmercapto)thiophene]. From Ref. [34].

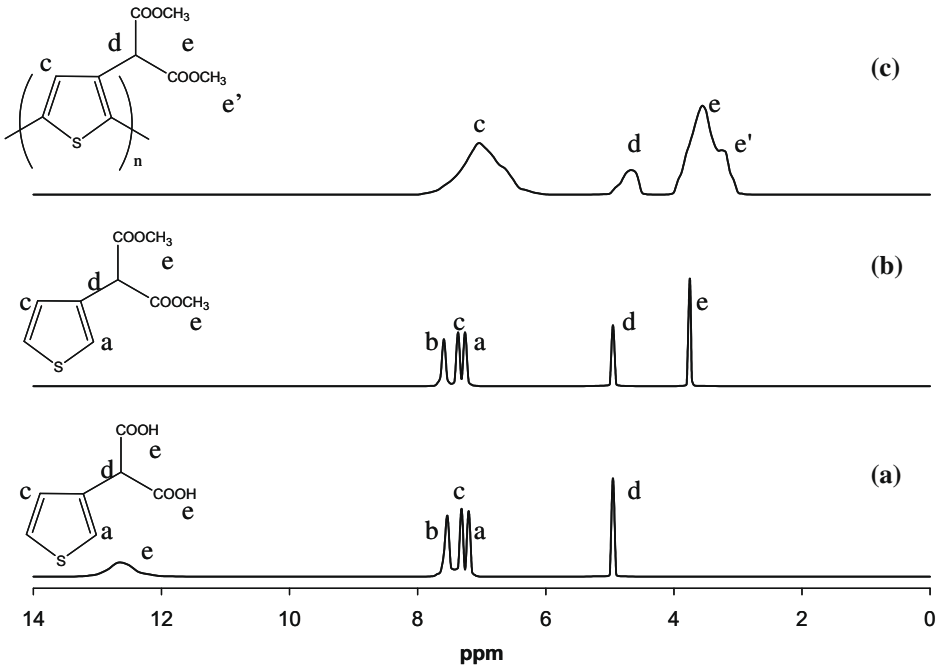

Fig. 2. ^1H NMR spectra of (a) T3MA and (b) T3MDE monomers and (c) PT3MDE polymer obtained from *d*-$CHCl_3$.

in the latter solvents was not altered upon heating. On the other hand, P3TMDE dissolve completely in organic solvents like toluene and dichloromethane.

The electrical conductivity was determined after doping with $FeCl_3$. Measurements were performed using two different types of samples. First, pellets of doped polymers were formed applying a pressure of 6 tons, the conductivity being determined using the standard four probe technique. The second type of samples was prepared applying a modification of the layer by layer polymerization-doping technique described in the literature [42], which involved the casting and doping of thin PT3MDE films on glass plates. A 10% weight polymer solution and 3M $FeCl_3$ solution in chloroform were used for this purpose. A thin film of dopant solution was placed on the deposited polymer layer and, subsequently, dried at room temperature. After this, the glass plates were washed with acetonitrile solution to remove the excess of ferric chloride. This procedure was repeated ten times, the average thickness of the resulting brown-black polymer films being 220 nm. The electrical conductivity on the resulting films was also determined using the four probe method.

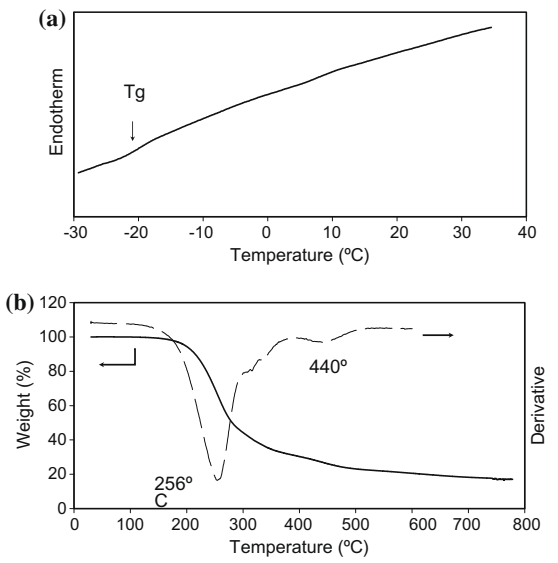

Fig. 3. (a) DSC heating run of PT3MDE: after fast cooling from the melt state (heating rate of 20 °C/min). The glass transition temperature is indicated by an arrow. (b) TGA curve of PT3MDE recorded at 20 °C/min of heating rate and from 30 to 700 °C of temperature range (dashed line: derivative curve).

The electrical conductivity obtained for doped PT3MDE was 6 S/cm. Although this value is one order of magnitude smaller than that previously measured for PT3AME, 15 S/cm [15], it is within the range typically determined for poly(3-alkylthiophene) derivatives [1]. On the other hand, the electrical conductivities determined on pressed pellets were lower than those obtained using films, which is consistent with the results obtained for other polythiophene derivatives [43]. The electrical conductivity of both the doped films and the pressed pellets decreased with time evidencing the sensitivity of this material towards the air.

3.5. Conformational analysis

In order to determine the conformation preferred by the malonic acid dimethyl ester substituent, quantum mechanical calculations on a T3MDE monomer were performed considering the all the possible arrangements of the dihedral angles χ, ξ and ξ' (Scheme 3). As each of these three dihedral angles was expected to exhibit three different minima, i.e. *trans* (180°), *gauche*$^+$ (60°) and *gauche*$^-$ (−60°), $3^3 = 27$ minima can be anticipated for the potential energy hypersurface (PEH) $E = E(\chi, \xi, \xi')$ of T3MDE. Full geometry optimization at the HF/6-31G(d,p) level of all these structures, which were used as starting points, led to six different minimum energy conformations. These structures are shown in Fig. 4, their dihedral angles and relative energies being also displayed. The driving force that defines the conformation of the substituent in all these structures is the minimization of the repulsive interactions between the four oxygen atoms. As the energy differences among the six minima obtained for the monomer are small, i.e. they are within a relative energy interval of 1.9 kcal/mol only, all these structures need to be considered for the construction of the dimers (hereafter denoted 2-T3MDE).

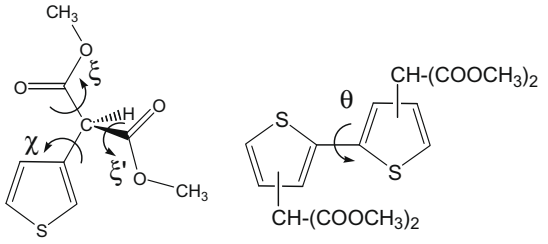

Scheme 3.

Calculations were performed to determine the relative stability and conformational preferences, in terms not only of the substituent arrangement but also of the inter-ring dihedral angle θ (Scheme 3), of the three possible isomers of 2-T3MDE. These isomers differ in the position of the substituent: 4,4′ (2-T3MDE$_{4,4'}$), 3,3′ (2-T3MDE$_{3,3'}$) and 3,4′ (2-T3MDE$_{3,4'}$), which represent the tail-to-tail (TT), head-to-head (HH) and head-to-tail (HT) polymer linkages, respectively. It is worth noting that the regiochemistry of polymer chains, which is defined during the polymerization process, depends on the attractive or repulsive interactions between monomeric units directly bonded. This allows predict the regiochemistry of polymer chains using simple models containing two monomeric units rather than complex models involving large polymer chains and/or intermolecular interactions.Results obtained for the T3MDE monomer indicated that each side group of 2-

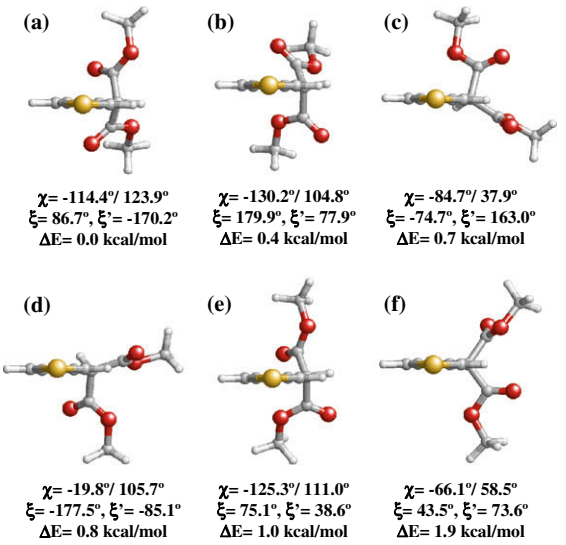

Fig. 4. Minimum energy conformation obtained for the T3MDE monomer after a systematic conformational search. Calculations were performed at the HF/6-31G(d,p) level. The dihedral angles of the side group and the relative energy (ΔE) of each minimum are also displayed. Dihedral angles have been defined as: $\chi = C_\alpha(Th)—C_\beta(Th)—C—C(=O)$ (the two complementary values are shown); ξ and $\xi' = C_\beta(Th)—C—C(=O)—O$ for the branch located above and below the ring, respectively. Th refers to the thiophene ring.

T3MDE may adopt six different arrangements (Fig. 4), which are expected to influence not only the inter-ring dihedral angle but also to the relative stability of the different isomers. Consideration of all these arrangements led to construct (2 minima for the internal rotation of θ: *anti-gauche* and *syn-gauche*) $\times$ ($\left[6^2 - \binom{6}{2}\right]$ arrangements of the two side chains) = 42 starting structures for the 2-T3MDE$_{4,4'}$ and 2-T3MDE$_{3,3'}$ isomers. The number of starting structures increased to $2 \times 6^2 = 72$ for the 2-T3MDE$_{3,4'}$ isomer since in this case substitution at positions 3,4′ and 4,3′ are not identical. Complete geometry optimization at the HF/6-31G(d,p) level led to 41, 8 and 45 minimum energy conformations for 2-T3MDE$_{4,4'}$, 2-T3MDE$_{3,3'}$ and 2-T3MDE$_{3,4'}$, respectively, i.e. 94 minima from an initial set of 156 structures.

Fig. 5 represents the distribution of the inter-ring dihedral angle θ against the relative energy, which has been calculated with respect to the lowest energy minimum of the most stable isomer, of all the minimum energy conformations identified for 2-T3MDE$_{4,4'}$, 2-T3MDE$_{3,3'}$ and 2-T3MDE$_{3,4'}$. As can be seen, the 2-T3MDE$_{4,4'}$ and 2-T3MDE$_{3,4'}$ isomers are practically isoenergetic. The former compound presents 23 minimum energy conformations within a relative energy interval of 1.5 kcal/mol, in 8 and 15 of them θ being arranged in *syn-gauche* (θ ranges from 41.9° to 45.9°) and *anti-gauche* (θ ranges from 145.6° to 148.8°), respectively. Thus, although the lowest energy minimum (Fig. 6a) of the 2-T3MDE$_{4,4'}$ isomer corresponds to an *anti-gauche* conformation, the lowest *syn-gauche* minimum (Fig. 6b) is destabilized by only 0.4 kcal/mol. Interestingly, the dihedral angles listed in Fig. 6a and b evidence that the side chains adopt the same arrangement in such two conformations, which corresponds to that found for the lowest energy conformation of the T3MDE monomer (Fig. 4).

Amazingly, the lowest energy minimum of the 2-T3MDE$_{3,4'}$ isomer corresponds to a *syn-gauche* minimum (Fig. 6c), no minimum with a typical *anti-gauche* conformation being detected for this dimer. Specifically, the repulsive interaction between the substituent attached to the C_3-position and the sulfur atom of the neighboring sulfur ring is very remarkable when $\theta \approx 150°$, a conformational change towards a distorted arrangement with $\theta \approx 110°$–120° (Fig. 5), being obtained in all geometry optimizations that started from a conventional *anti-gauche* conformation. However, all the structures, which are relatively close to the *gauche–gauche* conformation, are unfavored with the respect to the lowest energy minimum by more than 1.9 kcal/mol. Furthermore, all the minimum energy conformations detected within a relative energy interval of 1.5 kcal/mol, which were only 5, showed a *syn-gauche* conformation (θ ranging between 53.2° and 57.6°, the most stable minimum with a distorted conformation (Fig. 6d) being 1.8 kcal/mol destabilized with respect to the lowest energy minimum. As it can be seen, the minima displayed

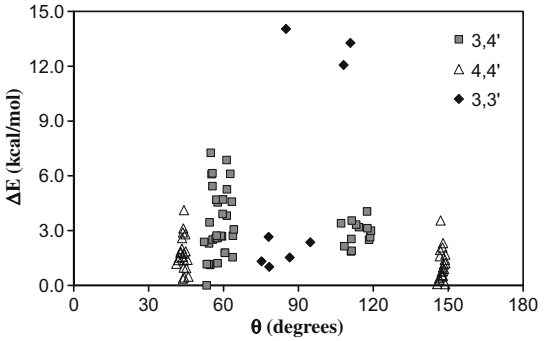

Fig. 5. Relative energy (ΔE), calculated with respect to the lowest energy arrangement of the most stable isomer, against the inter-ring dihedral angle (θ) of all the minimum energy conformations found for 2-T3MDE$_{4,4'}$, 2-T3MDE$_{3,3'}$ and 2-T3MDE$_{3,4'}$.

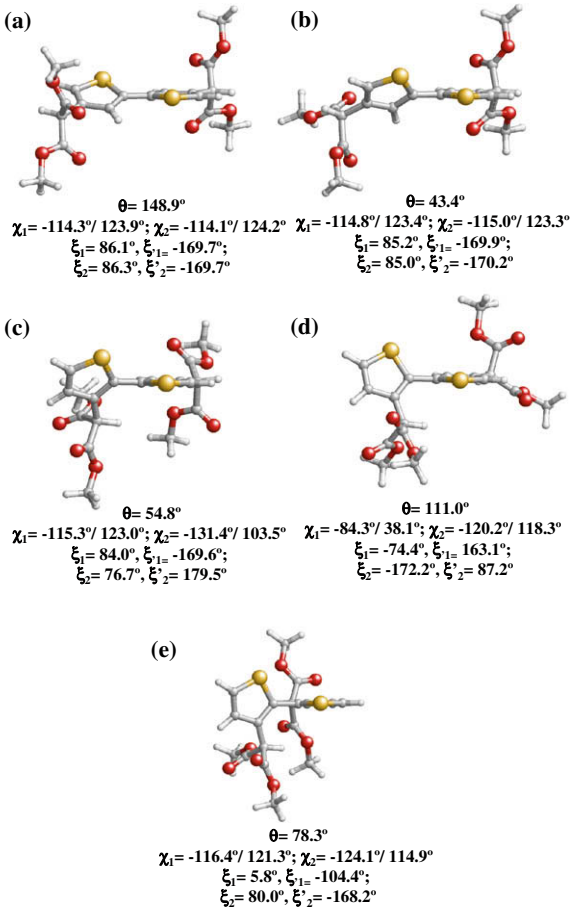

Fig. 6. Significant minimum energy conformation obtained for the 2-T3MDE$_{4,4'}$, 2-T3MDE$_{3,4'}$ and 2-T3MDE$_{3,3'}$ isomers after a systematic conformational search: (a) global minimum, in which θ shows an *anti-gauche* conformation, found for 2-T3MDE$_{4,4'}$; (b) lowest energy minimum with θ arranged in a *syn-gauche* conformation identified for 2-T3MDE$_{4,4'}$; (c) global minimum, in which θ shows a *syn-gauche* conformation, found for 2-T3MDE$_{3,4'}$; (d) lowest energy minimum with θ arranged in a distorted *anti-gauche* conformation identified for 2-T3MDE$_{3,4'}$; and (d) global minimum, in which θ shows a *gauche–gauche* conformation, found for 2-T3MDE$_{3,3'}$. Calculations were performed at the HF/6-31G(d,p) level. The inter-ring and side chain dihedral angles are listed for each minimum. Dihedral angles (see Scheme 3) have been defined as: θ = S—C—C—S; χ_i = C_α(Th)—C_β(Th)—C—C(=O) (the two complementary values are shown); ξ_i and ξ_i' = C_β(Th)—C—C(=O)—O for the branch located above and below the ring, respectively. Th refers to the thiophene ring while i = 1 or 2 indicates the first or second thiophene ring in the dimer, respectively.

in Fig. 6c and d differ in the conformation preferred by the side groups, which represents a significant difference with respect to the 2-T3MDE$_{4,4'}$ isomer.

In order to get more details about the high stability of the *syn-gauche* conformation predicted for this isomer, the potential energy curve of 2-T3MDE$_{3,4'}$ was calculated by scanning θ in steps of 15° between 0° and 360° and considering that the substituents are arranged like in the lowest energy minimum (Fig. 6c). The resulting energy profile, which was calculated using a flexible rotor approximation, i.e. each point of the path was obtained from a HF/6-31G(d,p) geometry optimization of the molecule at a fixed value of θ, is displayed in Fig. 7. Consistently, no minimum appears at the *anti-gauche*$^+$ and *anti-gauche*$^-$ conformations. Indeed, the three minima correspond to the *syn-gauche*$^+$ (θ = 53.2°) and *syn-gauche*$^-$ (θ = −62.1°), the latter being unfavored with respect to the former by 1.3 kcal/mol. These minima are separated by two barriers located at the *syn* (θ = 0°) and *anti* (θ = 180°) arrangements of 6.3 and 5.5 kcal/mol, respectively. Single point calculations at a higher level of theory, i.e. MP2/6-31G(d,p), provided very similar values for both the relative energy between the two minima (2.1 kcal/mol) and the lowest energy barrier (5.9 kcal/mol). On the other hand, it is worth noting that Fig. 7 shows flat regions that involve θ values ranging from 90° to 120° and, especially, from −120° to −90°. These structures show a kink arrangement similar to that of the local minima with a *gauche–gauche* conformation that were identified in Fig. 5.

Finally, the 2-T3MDE$_{3,3'}$ isomer was unfavored by 1.0 kcal/mol with respect to the other two because of the strong steric interactions induced by the substituents. The lowest energy minimum of this compound (Fig. 6e) corresponds to a *gauche–gauche* conformation. Indeed, the four minimum found within a relative energy interval of 1.5 kcal/mol adopt this conformation with θ values ranging from 75.2° to 94.8°. It is worth noting that in this isomer the repulsive interactions between the side groups are responsible of the annihilation of 34 of the 42 minima anticipated by the conformational analysis theory (Fig. 5).

Considering that the 2-T3MDE$_{3,4'}$ and 2-T3MDE$_{4,4'}$ isomers are isoenergetic while the 2-T3MDE$_{3,3'}$ is unfavored with respect to the other two, an idealized polymer chain constituted by consecutive HT linkages has been concluded to be favored with respect to a system formed by alternated HH and TT linkages. This is fully consistent with the distribution of diads found by ^{1}H NMR measurements (see above). In order to confirm the remarkable tendency of the HT polymer linkages to adopt a *syn-gauche* conformation, three trimers (3-T3MDE) were constructed for complete geometry optimization at the HF/6-31G(d,p) level. The side groups of these structures were arranged like in the lowest energy minimum of 2-T3MDE$_{3,4'}$ (Fig. 6c), while the inter-ring dihedral angles θ_1/θ_2 (Scheme 4) were arranged in *anti-gauche*/*anti-gauche* (trimer A) *anti-gauche*/*syn-gauche* (trimer B) and *syn-gauche*/*syn-gauche* (trimer C).

The results obtained for the trimers are summarized in Table 2. As can be seen, in all cases the substituent retained the initial arrangement independently of the values of the inter-ring dihedral angles. Trimer C showed the lowest energy, the other two conformations being unfavored by 1.4 (trimer B) and 1.9 kcal/mol (trimer A). These results evidence that, in order to reduce the repulsive steric interactions induced by the large size of the substituent, the inter-ring dihedral angles of PT3MDE prefer a *syn-gauche* conformation.

3.6. Calculation of the electronic properties

A model constituted by HT linkages was used to build oligomers containing *n* repeat units with *n* = 2, 3, 4, 5 and 6, which were optimized at the HF/6-31G(d,p) level. For each oligomer two different situations were considered: (i) optimizations were performed without any restriction using the *syn-gauche* conformation as starting point for all the inter-ring dihedral angles θ; and (ii) geometry optimizations were performed fixing the inter-ring dihedral angles at 180° (*anti* conformation). Previous studies indicated that, in order to extrapolate the electronic properties calculated for oligomers to infinite chain polymers, conformational effects should be omitted by imposing an all-*anti* conformation [24,44]. However, in this case the latter conformation has been found to be strongly destabilized due to the large size of the substituent. Specifically, the all-*syn-gauche* conformation, hereafter denoted all-*sg*, is favored with respect to the all-*anti* by 4.5 kcal/mol per repeat unit at the HF/6-31G(d,p) level. The all-*sg* (complete geometry optimization) and all-*anti* (restricted geometry optimization) obtained for the oligomer with *n* = 6 are compared in Fig. 8. As can be seen, complete minimization of the repulsive interactions induced by the side groups produce significant conformational distortions in the backbone.

In order to evaluate the ε_g and IP of PT3MDE, single point calculations at the B3PW91/6-31G(d,p) level were

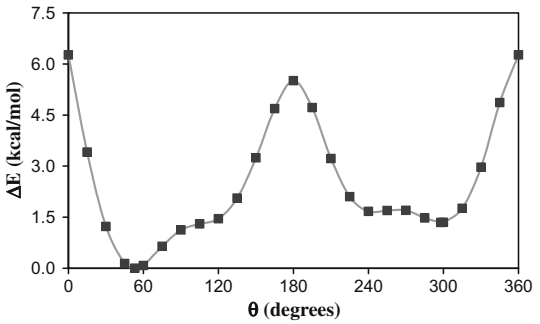

Fig. 7. Potential energy curve for the internal rotation as a function of the inter-ring dihedral angle (θ) of 2-T3MDE$_{3,4'}$ using HF/6-31G(d,p) optimizations. Energies are relative to the global minimum.

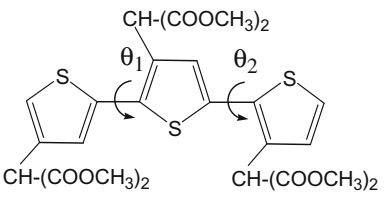

Scheme 4.

Table 2
Relative energy (ΔE) and inter-ring dihedral angles[a] (θ_1 and θ_2; see Scheme 4) and dihedral angles[a] of each substituent[b] (χ_i, ξ_i, ξ'_i with i = 1, 2 and 3) for the three conformation of 3-T3MDE (see text) optimized at the HF/6-31G(d,p) level.

	Trimer A	Trimer B	Trimer C
ΔE (kcal/mol)	1.9	1.4	0.0
θ_1	149.1	145.7	52.1
θ_2	−117.0	−68.1	52.3
χ_1	−116.0/122.1	−114.7/123.4	−113.8/124.7
χ_2	−132.0/102.8	−119.9/118.6	−116.4/122.1
χ_3	−130.5/107.8	−114.7/123.4	−118.5/119.9
ξ_1, ξ'_1	86.3, −170.7	87.0, −171.0	80.4, −169.5
ξ_2, ξ'_2	74.4, −177.1	79.8, −167.2	81.9, −170.8
ξ_3, ξ'_3	62.1, −166.0	85.0, −169.4	87.4, −170.6

[a] In degrees.
[b] The dihedral angles χ_i, ξ_i and ξ'_i (see Scheme 3) have been labeled as a function of the position of the substituent in the first (i = 1), second (i = 2) and third (i = 3) ring.

performed on the optimized geometries of all the oligomers. Fig. 9 shows the linear behavior (correlation coefficient $r > 0.99$) for the variation of the calculated ε_g and IP with the inverse chain length ($1/n$) for both the all-*sg* and all-*anti* conformations. Linear regression analyses, which are also displayed in Fig. 9, allowed extrapolate ε_g/IP values of 3.75/5.40 and 2.38/4.71 eV for an infinite chain of PT3MDE that adopts an all-*sg* and all-*anti* conformation, respectively. As can be seen, the dependence of these two electronic properties on the polymer conformation is very strong. Thus, the variation of the relative arrangement between consecutive thiophene rings from *anti* to *syn* and the loss of planarity (from *syn* to *syn-gauche*) increase the ε_g and the IP by 1.37 and 0.69 eV, respectively.

Comparison of the ε_g predicted for PT3MDE chain with that calculated for related conducting polymers using a similar theoretical level and an idealized all-*anti* conformation, e.g. PT3AME (2.28 eV) [15], poly(3-thiophene-3-yl acrylic acid) (2.12 eV) [16], PT3AA (2.12 eV) [16], poly(3-thiopheneformic acid) (1.99 eV) [31] and polythiophene (1.82 eV) [31], clearly indicates that the bulky side group is responsible not only of the drastic geometrical distortions showed above but also of the significant increase of the lowest transition energy, which should be related with a detriment of the optical and electrical properties.

The ε_g derived from the UV–vis spectrum recorded for PT3MDE in acetone (not shown) is 2.75 eV. This value is 0.21 and 0.30 eV higher than that determined in the same solvent for PT3AME (2.54 eV) [15] and PT3AA (2.45 eV) [16], respectively, confirming the theoretical predictions reported above. On the other hand, the experimental gap is 1.00 eV lower than that predicted by quantum mechanical calculations for an idealized chain that adopts an all-*sg* conformation and 0.37 eV higher than that calculated for a chain arranged in a perfect all-*anti*. Considering that B3PW91/6-31G(d,p) method is able to reproduce quantitatively the ε_g values of polythiophene derivatives

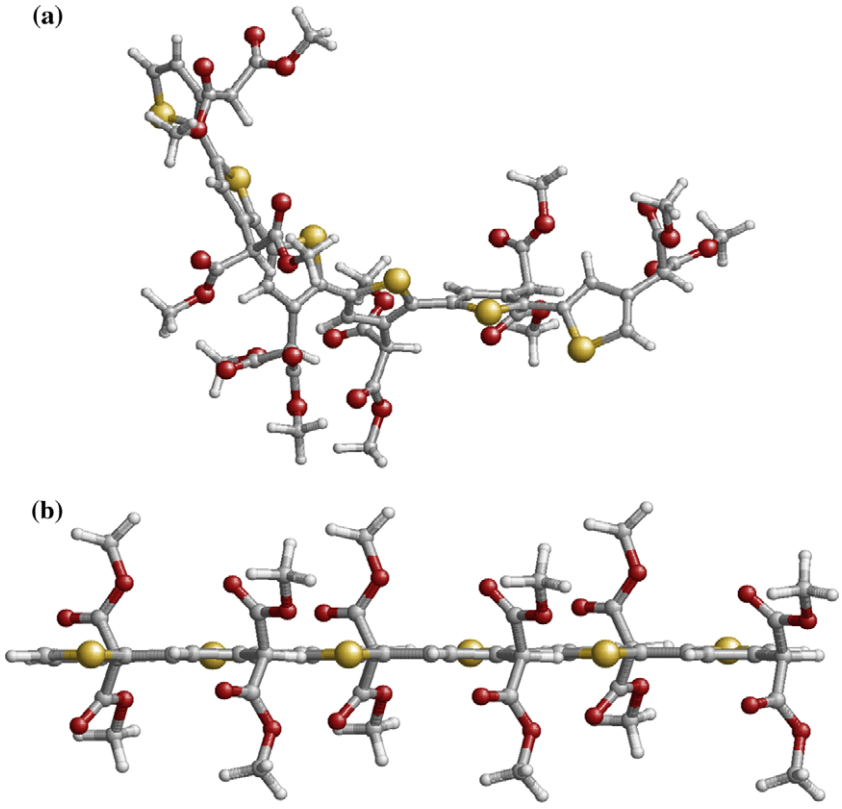

Fig. 8. Molecular structures obtained for 6-T3MDE after (a) complete geometry optimization of using the all-*syn-gauche* conformation as starting point and (b) restricted geometry optimization of the all-*anti* conformation.

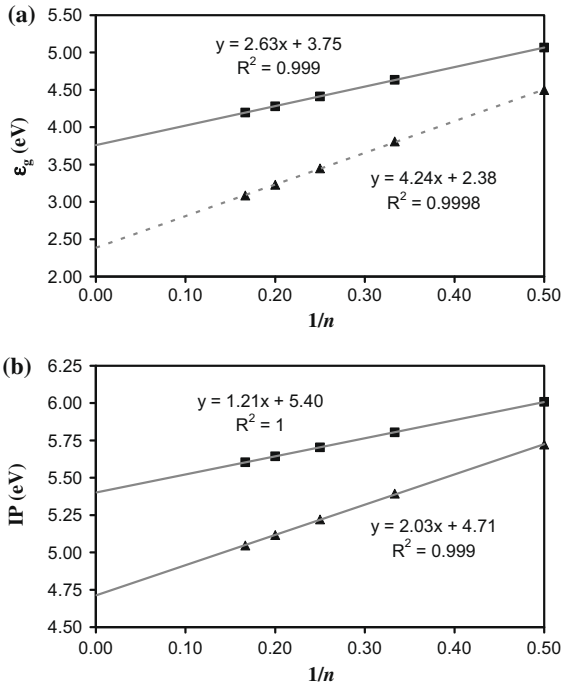

Fig. 9. Variation of (a) ε_g (in eV) and (b) IP (in eV) against $1/n$, where n is the number of repeat units, for PT3MDE arranged in all-*anti* (triangles) and all-*syn-gauche* (squares) conformations. The gray lines correspond to the linear regressions used to obtain the values of these electronic properties for infinite chain systems.

[15,16,22,31,32], the difference between the experimental and theoretical estimations should attributed to the following features: (i) the lack of HH/TT couplings, which were found to contribute 25% by ^{1}H NMR, in the molecular model used for the theoretical calculations; (ii) the omission of environmental effects on the *syn-gauche*, *anti-gauche* and *anti* conformations, i.e. previous studies on 2,2′-bithiophene evidenced that organic solvent affect the relative stability of these conformations [45]; and (iii) the absence of conformational variability in our theoretical model, which has been constructed using identical repeating units, i.e. different conformational states (for both the backbone and the side groups) are expected to be present according to their Boltzmann probabilities in a realistic polymer chain, especially in solution.

4. Conclusions

PT3MDE, a new polythiophene derivative with a polar side group, has been prepared by chemical oxidative-coupling polymerization. The chemical structure of this material has been studied using FTIR and ^{1}H NMR spectroscopy. Interestingly, the electrical conductivity of PT3MDE (6 S/cm), which is solute in non-polar and polar organic solvents, is higher than that typically found for poly(3-alkylthiophene) derivatives. However, PT3AME, a related polymer in which the ester arises from acrylic acid, showed an electrical conductivity (15 S/cm) that was higher by one order of magnitude. The different electrical behavior between PT3MDE and PT3AME can be explained by conformational preferences of the inter-ring dihedral angles and the flexibility of the side group. Thus, the latter feature was evidenced not only by ab initio quantum mechanical calculations but also the glass transition temperature, which was higher for PT3AME than for PT3MDE.

A systematic conformational analysis considering the T3MDE monomer, the three isomers of the 2-T3MDE dimer and selected conformations of the 3-T3MDE trimer, allowed to conclude that the most stable model for an idealized polymer chain corresponds to that obtained by repeating HT linkages, which is in complete agreement with the regiochemistry determined by ^{1}H NMR measurements. Furthermore, the inter-ring dihedral angles tend to adopt a *syn-gauche* conformation that allows minimize the repulsive interactions induced the bulky side groups. This represents a significant difference with respect to conventional substituted polythiophene derivatives for which the *anti-gauche* conformation was preferred.

Calculation of the electronic properties on idealized oligomers ideally formed by HT linkages revealed that both the ε_g and the IP strongly depend on the backbone conformation. In spite of the drastic approximations applied in the construction of the molecular model used for the calculations, the ε_g value predicted for PT3MDE is in good agreement with the experimental estimation. Both quantum mechanical calculations and the UV–vis spectrum indicate that the gap of PT3MDE is significantly higher than that obtained for other substituted polythiophene derivatives. This detriment is consequence of the geometrical distortions induced by the bulky side group in the polymer backbone.

Acknowledgements

This work has been supported by MCYT and FEDER with Grant MAT2006-04029. Authors are indebted to the Centre de Supercomputació de Catalunya (CESCA) for computacional facilities. Support for the research of C.A. was received through the prize "ICREA Academia" for excellence in research funded by the Generalitat de Catalunya.

References

[1] Chan HSO, Ng SC. Prog Polym Sci 1998;23:1167.
[2] Roncali J. Chem Rev 1997;97:173.
[3] Barbarella G, Melucci M, Sotgiu G. Adv Mater 2005;17:1581.
[4] Sato M, Tanaka S, Kaeriyama K. J Chem Soc Chem Commun 1986;873.
[5] Jen KY, Miller GG, Elsenbaumer RL. J Chem Soc Chem Commun 1986;1346.
[6] Bryce MR, Chissel A, Kathirgamanathan P, Parker D, Smith NRM. J Chem Soc Chem Commun 1987;6:466.
[7] Patil OA, Ikenoue Y, Wudl F, Heeger AJ. J Am Chem Soc 1987;109:1858.
[8] Chayer M, Fa K, Leclerc M. Chem Mat 1997;9:2902.
[9] Masuda H, Kaeriyama K. Makromol Chem Rapid Commun 1992;13:461.
[10] Kim B, Chen L, Gong J, Osada Y. Macromolecules 1999;32:3964.
[11] Liaw DJ, Liaw BY, Gong JP, Osada Y. Synth Met 1999;99:53.
[12] Welzel HP, Kossmehl G, Stein HJ, Schneider J, Plieth W. Electrochim Acta 1995;40:577.
[13] Visy C, Kankare J, Kriván E. Electrochim Acta 2000;45:3851.
[14] Ewbank PC, Loewe RS, Zhai L, Reddinger J, Sauvé G, McCullough RD. Tetrahedron 2004;60:11269.
[15] Bertran O, Pfeiffer P, Torras J, Armelin E, Estrany F, Alemán C. Polymer 2007;48:6955.

[16] Bertran O, Armelin E, Torras J, Estrany F, Codina M, Alemán C. Polymer 2008;49:1972.
[17] Teixeira-Dias B, del Valle LJ, Estrany F, Armelin E, Oliver R, Alemán C. Eur Polym J 2008;44:3700.
[18] Alemán C, Teixeira-Dias B, Zanuy D, Estrany F, Armelin E, del Valle LJ. Polymer 2009;50:1965.
[19] Pfeiffer P, Armelin E, Estrany F, del Valle LJ, Cho LY, Alemán C. J Polym Res 2008;15:225.
[20] Hariharan PC, Pople JA. Chem Phys Lett 1972;16:217.
[21] Alemán C, Domingo V, Ll Fajarí, Julià L, Karpfen A. J Org Chem 1998;63:1041.
[22] Alemán C, Casanovas J. J Phys Chem A 2004;108:1440.
[23] Ocampo C, Curcó D, Alemán C, Casanovas J. Synth Met 2006;156:602.
[24] Alemán C, Julià L. J Phys Chem 1996;100:1524.
[25] Koopmans T. Physica 1934;1:104.
[26] Gatti C, Frigerio G, Benincori T, Brenna E, Sannicolò F, Zotti G, et al. Chem Mater 2000;12:1490.
[27] Alemán C, Armelin E, Iribarren JI, Liesa F, Laso M, Casanovas J. Synth Met 2005;149:151.
[28] Becke AD. J Chem Phys 1993;98:1372.
[29] Perdew JP, Wang Y. Phys Rev B 1992;45:13244.
[30] Frich MJ, Pople JA, Krishnam R, Binkley JS. Chem Phys 1984;80:3264.
[31] Casanovas J, Zanuy D, Alemán C. Polymer 2005;46:9452.
[32] Casanovas J, Alemán C. J Phys Chem C 2007;111:4823.
[33] Janak JF. Phys Rev B 1978;18:7165.
[34] Levy M, Nagy A. Phys Rev A 1999;59:1687.
[35] Frisch MJ, et al. Gaussian 03, Revision B.02. Pittsburgh PA: Gaussian, Inc.; 2003.
[36] Yoshino K, Nakao K, Onoda M, Sugimoto R. Solid State Commun 1989;70:609.
[37] Ruiz JP, Kayak K, Marynick DS, Reynolds JR. Macromolecules 1989;22:1231.
[38] Haslam J, Willis HA. Identification and analysis of plastics. 2nd ed. Iliffe Books Ltd. Ed.; 1967. p. 28.
[39] Welzel HP, Kossmehl G, Schneider J, Plieth W. Macromolecules 1995;28:5575.
[40] Skotheim TA, Reynolds JR. In: Handbook of Conducting Polymers. Boca Raton: CRC Press; 2007.
[41] Bjerring M, Nielsen JS, Nielsen NC, Krebs FC. Macromolecules 2007;40:6012.
[42] Nicolau YF, Daried S, Genoud F, Nechtschein M, Travers JP. Synth Met 1991;42:1491.
[43] Chayer M, Faid K, Leclerc M. Chem Mater 1997;9:2902.
[44] Ocampo C, Casanovas J, Liesa F, Alemán C. Polymer 2006;47:3257.
[45] Rodríguez-Ropero F, Casanovas J, Alemán C. Chem Phys Lett 2005;416:331.